

Received September 15, 2019, accepted October 9, 2019, date of publication October 11, 2019, date of current version October 24, 2019.

Digital Object Identifier 10.1109/ACCESS.2019.2946989

# On MAC Access Delay Distribution for IEEE 802.11p Broadcast in Vehicular Networks

YUAN YAO<sup>1</sup>, (Member, IEEE), YUJIAO HU<sup>1</sup>, (Student Member, IEEE),  
GANG YANG, (Member, IEEE), AND XINGSHE ZHOU, (Member, IEEE)

School of Computer Science, Northwestern Polytechnical University, Xi'an 710072, China

Corresponding author: Yuan Yao (yaoyuan@nwpu.edu.cn)

This work was supported in part by the National Natural Science Foundation of China under Grant 61751208, Grant 61876151, Grant 61502394, and Grant 61972318, and in part by the Fundamental Research Funds for the Central Universities under Grant 3102019DX1005.

**ABSTRACT** The inter-vehicle safety communication is generally considered as a promising technology to significantly enhance road safety. In fact, a lot of communications about inter-vehicle safety have real-time, rigorous requirements on broadcast messages in order to make sure that drivers have sufficient time for reaction towards emergencies. The procedure of the control for medium access is of significance for the delay-constrained communication systems. Therefore, in-depth investigation should be conducted for IEEE 802.11p covering the MAC and PHY protocol. Nonetheless, most existing studies only focus on the average delay analysis that includes insufficient information of inter-vehicle communications' real capacity. So as to evaluate the single-hop broadcast's performance under 802.11p, an analytical model is put forward in this paper. Both of simulation and real-world experiment results indicate that our model accurately estimates the probability distribution, deviation and mean of the MAC access delay. In addition, it can be proved that exponential distribution can be a good approximation to the distribution of MAC access delay with the usage of the K-S test. With such observation, it is convenient for us to conduct an analysis on the queuing delay in the MAC layer. As shown by the numerical analysis, the support of QoS in 802.11p provides sound guarantee about performance for higher priority messages. However, it cannot meet the real-time requirement of the applications with lower priority.

**INDEX TERMS** DSRC, IEEE 802.11p, MAC access delay, safety communications, vehicular ad hoc networks.

## I. INTRODUCTION

Vehicle-to-Vehicle (V2V) safety communication is a key technology for the future Intelligent Transportation System (ITS). The typical safety applications include electronic brake lights for emergency, cooperative forward collision warning, assistance of lane change, assistance for intersection movement, notification for hazardous location, warning of blind spot and so forth [1]. As shown by a report, 79% of vehicle crashes can be greatly decreased by the systems of V2V [2]. Nonetheless, the safety-related applications heavily rely on the delivery of real-time message. The communication latency should be minimized to ensure that drivers have sufficient time to handle emergencies. Commonly, these safety messages require direct communication between

nearby vehicles. Thus, the broadcast mode is adopted by a majority of V2V safety applications [3].

MAC protocol design is very significant for the time-critical applications. The backoff procedure, retransmission scheme and QoS support can greatly impact the delay performance in the MAC-layer. IEEE 802.11p<sup>1</sup> adopts the contention-based Carrier Sense Multiple Access (CSMA) mechanism, which has unpredictable delay if the system gets heavy load. Therefore, the IEEE 802.11p MAC protocol's performance has been studied by lots of researchers so as to find out how severe the MAC access delay in the typical

<sup>1</sup>In order to enhance the performance of DSRC, a new Study Group called the IEEE 802.11 Next Generation V2X (NGV) was formed in March 2018. NGV aims to develop a new IEEE Task Group IEEE 802.11bd [4] which requires to be backward compatible with 802.11p. Since IEEE 802.11bd is currently under development, in this paper, we do not discuss this standard amendment until the new features and functionalities are determined in the final version.

The associate editor coordinating the review of this manuscript and approving it for publication was Arun Prakash<sup>1</sup>.

safety communication scenario. Most of them regard the delay of MAC access in the environment of VANET [5]–[7]. However, the practical situation of the safety communication cannot be fully reflected by the mean value. The cases of the large latency might occur due to the stochasticity of the scheme of IEEE 802.11p MAC although the mean delay is less than the deadline.

Actually, designers can benefit more from the distribution of the random variable of access delay. Therefore, this paper is intended to build an analytical model so as to obtain the MAC access delay distribution of the standard IEEE 802.11p. First of all, a two-dimensional highway model is leveraged to describe the vehicle distribution on the road. Then, to calculate the above important ranges in vehicular communications, a dual-slope propagation model measured in a real DSRC radio platform is adopted in this paper, unlike most works assuming the range of carrier sensing, the fixed range of transmission, as well as the range of interference. Finally, to study the distribution of delay in the broadcast mode, two Markov Chains for ACs with different priorities are adopted. As shown by the simulation result, the probability distribution, deviation and mean of the analytical model is of high accuracy. Besides, it can be observed that a shifting exponential distribution is closely related to the distribution of MAC access delay. With this observation, we can further analyze the queuing delay of the MAC-layer. In fact, lots of studies have shown that when IEEE 802.11p with QoS support cannot assure the real-time demand of the applications with lower priority, it can offer sound performance to the messages with higher priority.

The main contributions of this paper are three-fold:

- An analytical model is established to evaluate the MAC access delay distribution of the standard IEEE 802.11p protocol in a vehicular communication environment. The proposed model can be utilized to obtain the explicit expressions of the distribution of MAC access delay.
- To calculate the important ranges in vehicular communications, a dual-slope propagation model is used, unlike most of works which only assume the fixed range of transmission, the range of carrier sensing as well as the range of interference.
- Two Markov Chains for ACs with different priorities in MAC queue is employed to analyze the delay distribution for different QoS requirements.

Below is the structure of the rest of the paper. Related works are provided in Section II. Section III provides an overview of wireless protocol for the communication of VANET and V2V safety in a highway environment. Section IV shows the analytical model and derives the probability distribution, deviation and mean of the MAC access delay from the view of a particular tagged node. The proposed model is validated by both the network simulation and field test in Section V. And numerical results are analyzed in Section VI. Finally, Section VII draws the conclusion.

## II. RELATED WORK

Bianchi [8] first proposed the Markov Chain for the modeling of the IEEE 802.11 MAC protocol, and lots of studies further analyze other standards of the 802.11 series by improving this accurate model. Most of the active researches on the performance analysis on the broadcast of the safety message only consider the mean delay metric. To evaluate the packet reception rate and packet delay of the V2V safety-related broadcast services. Ma *et al* [6] put forward a one-dimensional Markov chain model. It illustrates that the direct broadcast mode can meet the delay requirement of the safety applications. Ramakrishnan *et al.* [7] conducted simulation in the C++ platform to analyze the performance with practical vehicle distribution. It shows that the packet delay of 802.11p is only tens of milliseconds. However, these analyses are based on the mean MAC access delay which may not reflect the real situation. Since the MAC scheme in IEEE 802.11p has great randomness, a conclusion can be easily drawn that although the mean delay is not big, it meets the real-time demand. Indeed, the distribution of the random variable has more practical meanings for the designers.

A number of studies have been conducted to study the MAC access delay distribution of the messages about IEEE 802.11p safety broadcasted via evaluation [9], [11]. And in simulations, the saturated and non-saturated conditions are studied respectively. Nevertheless, they adopt the two-ray ground propagation model which is impractical in vehicular communication environment. Pramuanyat *et al.* [12] utilized the long-distance propagation loss model in the simulations and evaluated the MAC access delay in the testbed composed of DENSO WSU. However, the explicit expressions of MAC access delay cannot be obtained.

Some studies have modeled the MAC access delay distribution based on 802.11b DCF. In addition, Wang *et al.* [13] used the signal transfer function to generate a probability distribution of the MAC access delay in IEEE 802.11b and used Markov chain to model the exponential process of backoff. Uddin *et al.* [14] adopted the Rayleigh fading and shadowing propagation model to obtain explicit expression for the distribution, standardized deviation and mean of the MAC access delay. It is approved that a condensed power-law tail is included in the distribution when there is a limit of retransmission while a heavy-tailed delay distribution for unlimited retransmission is induced by the binary exponential backoff mechanism. Nonetheless, the model has a single kind of message under the indoor environment into account. Pend *et al.* [15] introduced an IEEE 802.11p-based communication model for multiplatooning scenarios. They presented a performance analysis of DCF-based intra- and inter-platoon communications and derived expression for packet delay. However, these models are not suitable for the multi-priority messages in the VANET environment.

In order to assess multi-traffic's MAC delay with various kinds of QoS support, Han *et al.* [16] put forward the analytical models for the IEEE 802.11p EDCA under saturated

TABLE 1. Comparison of different solutions.

Research	Protocol	Propagation	MAC Type	Network Condition	Method	Validation	Year
Bianchi [8]	802.11	-	DCF	S	M	S	2000
Ma [6]	802.11a	-	DCF	N-S/S	M	S	2009
Martelli [9]	802.11p	Two-Ray Ground Model	EDCA	S	E	S	2012
Salahuddin [10]	802.11p	-	EDCA	S	M	S	2014
Kolici [11]	802.11p	Two-Ray Ground Model	EDCA	N-S	E	S	2015
Pramuanyat [12]	802.11p	Log-distance Propagation Loss Model	EDCA	N-S/S	E	S/E	2015
Wang [13]	802.11b	-	DCF	N-S/S	M	S	2015
Uddin [14]	802.11b	Rayleigh Fading and Shadowing Model	DCF	N-S/S	M	S	2016
Peng [15]	802.11p	-	DCF	N-S/S	M	S	2017
Han [16]	802.11p	-	EDCA	N-S	M	S	2012
Xu [17]	802.11p	-	EDCA	N-S/S	M	S	2016
Zheng [18]	802.11p	-	EDCA	N-S/S	M	S	2016
Hu [19]	802.11p	-	EDCA	N-S/S	M	S	2017
Noor-A-Rahim [20]	802.11p	Measurement-based Path Loss and Fading Model	EDCA	N-S/S	M	S	2018
Our work	802.11p	Measurement-based Dual-slop linear model	EDCA	N-S/S	M/E	S/E	2019

Note: Network Condition (N-S/S): Non-Saturated/Saturated, Method (M/E): Model/Evaluation, Validation (S/E): Simulation/Experiment

network condition. Actually, unsaturated conditions tend to be more common in the VANET environment. Some other works [17]–[19] proposed the analytical models for IEEE 802.11p EDCA under both saturated and unsaturated network condition. Noor-A-Rahim et al. [20] presented an analytical model for IEEE 802.11p EDCA which is applicable for the different positions of transmitters and receivers in the intersection areas. However, all these models do not analyze the MAC access delay distribution.

So far, very limited work has been conducted to obtain explicit expressions of the MAC access delay distribution of IEEE 802.11p EDCA which is broadcasted in a theoretical way. In addition, most models neglect the propagation model that assumes fixed transmission, carrier sensing and interference ranges. Furthermore, the models are not validated by both simulations and experiments. A detailed comparison of previous works and our solutions is shown in Table 1.

### III. WIRELESS PROTOCOL FOR VEHICULAR SAFETY COMMUNICATION

The wireless protocol stack for vehicular communications as well as the design details of the IEEE 802.11p are introduced in this section in order to illustrate the differences between IEEE 802.11p MAC protocol and other 802.11 series protocols. Subsequently, differentiation parameters and the backoff procedure of IEEE 802.11p EDCA scheme are elaborated. Finally, we show the features of the V2V safety communication and provide a one-dimensional model for the typical highway environment.

#### A. AN OVERVIEW OF WIRELESS PROTOCOL FOR THE VEHICULAR ENVIRONMENT

WAVE standard means the wireless access in the vehicular environment. As a protocol stack is intended for the

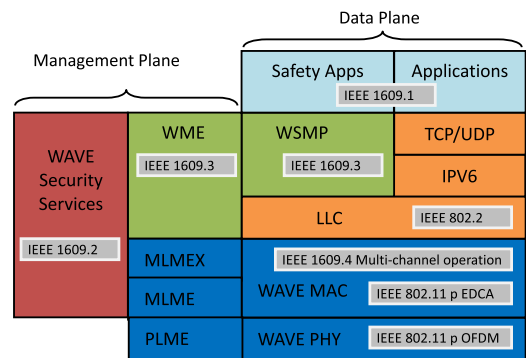


FIGURE 1. WAVE protocol stack.

high-speed vehicular environment, it consists of a series of standards of IEEE 1609 and IEEE 802.11p. Figure 1 indicates the protocol stack of WAVE.

The communications of Vehicle-to-infrastructure (V2I) and Vehicle-to-Vehicle (V2V) are supported by the WAVE stack. It is constituted of IEEE 802.11p as well as a standard family 1609, in which the upper layers are defined by IEEE 1609 and link layer and physical layer are covered by IEEE 802.11p. IEEE 1609.1 defines the resource management at the application layer. The Resource Command Processor (RCP) in On-board Unit (OBU) as the user requests service from the remote host whereas the Resource Manager (RM) in the Road-Side Unit (RSU) provides service. IEEE 1609.3 implements the WSMP for both transport protocol and network. IEEE 1609.2 considers the safety issues. The operations with multiple channels for upper layers are enabled by IEEE 1609.4.

IEEE 802.11p included in WAVE stack is a new amendment of IEEE 802.11 series for vehicular wireless communication according to the spectrum of Dedicated Short-Range

Communication (DSRC). The latest version of IEEE 802.11p has been published in July 2010 after obtaining approval [21]. The physical layer will use the modulation scheme of Orthogonal Frequency Division Multiplex (OFDM) that is similar to the standard of IEEE 802.11a. It introduces some changes to parameters, such as the bandwidth, symbol duration and subcarrier spacing. Subsequently, the range of transmission rate is from 3 to 27 Mbps which is 50% of the bandwidth in IEEE 802.11a. To support the Quality of Service (QoS) from IEEE 802.11e, Enhanced Distributed Channel Access (EDCA) is adopted in the MAC layer.

The basic channel access mechanism follows the EDCA that allows higher priority applications to occupy the channel with shorter Arbitration Inter-Frame Space (AIFS). Nevertheless, multi-channel operations on seven IEEE 1609.4-defined channels with the 10-MHz width should be provided by IEEE 802.11p.

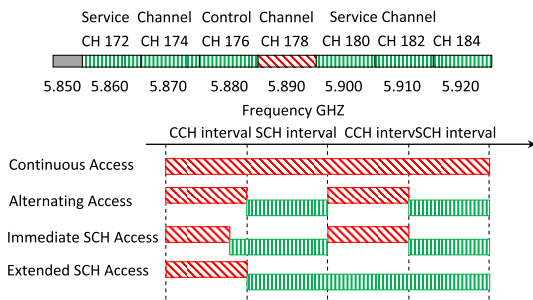


FIGURE 2. Multi-channel operation.

Figure 2 shows that the central Control Channel (CCH) is only for the dissemination of common safety messages. The remaining six are Service Channel (SCH) for the non-safety applications. The channel time can be divided in alternating CCH interval and SCH interval in IEEE 1609.4. Each interval is 50ms so that the CCH interval can be scheduled ten times per second. The interval long meets the requirement of the 10HZ safety message rate. Four channel access options, including continuous access, alternating access, immediate SCH access and extended SCH access are provide by IEEE 1609.4. Nevertheless, only the former two access schemes can support the timely safety message dissemination. The mode of continuous access mode is the highlight of this paper, as the mode can provide the best delay performance for the broadcast of safety message.

**B. EDCA DIFFERENTIATION PARAMETERS AND BACKOFF PROCEDURE**

So as to offer QoS support, IEEE 802.11p adopts EDCA as the channel access mechanism. A node has four access categories (ACs) with various priorities. Every AC is as an improved DCF with a MAC queue entity differentiated by the parameters of channel access, including Transmission Opportunity (TXOP), Contention Window (CW) and Arbitration Inter-Frame Space (AIFS). AC0 signifies the highest priority whereas AC3 signifies the lowest priority in the definition of IEEE 802.11p protocol.

For the AC<sub>i</sub>, let  $W_{i,j}$  be the  $j^{th}$  retransmission, i.e. the  $j^{th}$  backoff stage. Let  $CW_{i,max}$  be the maximum size of contention window and  $CW_{i,min}$  be the initial size of backoff window. The relationship among  $W_{i,j}$ ,  $CW_{i,min}$  and  $CW_{i,max}$  are shown as below:

$$W_{i,j} = \begin{cases} \gamma_i^j W_{i,0}, & j \leq M_i \\ \gamma_i^{M_i} W_{i,0}, & M_i < j \leq L_i \end{cases} \quad (1)$$

where,  $M_i = \log_{\gamma_i} (CW_{i,max}/CW_{i,min})$  refers to the maximum times doubled by the CW of AC<sub>i</sub>,  $\gamma_i$  is the window-increasing factor commonly defined as 2. and  $L_i$  refers to the retry limit of the AC<sub>i</sub> backoff. Different ACs have the same retry limit without the loss of generality. Therefore,  $L_i$  is denoted by  $L$  in this paper.

If the channel is idle, EDCA and DCF have different defer time. When the channel is idle for a constant Distributed Inter-Frame Space (DIFS), DCF allows a node to transmit packets. On the other hand, ACs access channel by differentiating different defer time AIFS. It has a better chance to earlier access channel when AC has smaller AIFS.

When the channel is occupied by an AC entity, the limit of TXOP enables the consecutive transmissions of packets. Nevertheless, IEEE 802.11p has not defined TXOP.

Four AC queues are implemented in one node, and each queue behaves roughly as the DCF entity. The higher-layer frames reach the layer of MAC with various priorities, and subsequently arrive at various queues. In a node, the backoff instances can be regarded as independent of each other with no virtual collision. For every AC, the channel transmits when it is sensed idle for the time which is equal to an AIFS. If not, AC will continue to monitor the channel till the time of idle reaches AIFS when the channel is busy. Herein, each AC can generate a random interval based on the value of CW and starts a backoff process. The backoff counter reduces if the channel continues to be idle for a time period of AIFS. The node of destination sends back the frame of ACK to the source node when it gets the delivery, and the source node might become idle or transmit a next frame. Another backoff procedure with double CW is invoked for the failure of transmission incurred by external collision when the source node cannot get ACK in a timeout of ACK which has been previously defined. CW will be doubled till it arrives at  $CW_{max}$  or the number of retransmissions reaches the retry limit after every unsuccessful transmission. This paper only focuses on the delay of packets received at the layer of MAC successfully.

Nonetheless, due to the internal virtual collisions, in a station, various backoff instances cannot completely and independently access the channel.

**C. V2V SAFETY COMMUNICATION IN A HIGHWAY ENVIRONMENT**

The communication of V2V safety is to exchange status information and emergency between nearby vehicles to avoid crashes. The safety applications usually require direct

interactions with surrounding vehicle. Thus, in consideration of the low delay limit and dynamic topology, the single-hop broadcast on CCH is used to inform neighboring vehicles with safety messages. VANET has two kinds of safety messages. One is the messages about routine safety (or time-triggered messages). Each vehicle periodically broadcasts such type of messages containing its velocity, location, direction as well as other detail attributions, such as the size and length of the vehicle, the control of acceleration, and so forth. Routine safety messages can enhance one vehicle’s understanding about the surrounding environment and enable drivers to predict the potential dangers. The other one is event-driven messages (the messages about emergent safety) that are sent while abnormal situation or danger can be detected. Such kind of messages relates to the applications of safety. Jiang *et al.* [22] provides an example to illustrate how these messages can help avoid crashes. In order to assure the up-to-date information, the messages about routine safety are sent with the frequency of 10Hz whereas the messages about emergent safety are occasionally generated yet a guaranteed, fast transmission is needed. Thus, routine messages have lower priority than such kind of messages. As shown in Figure 3, in the first scenario, vehicle A slows down and broadcasts its status. Based on the information, vehicle B can pass vehicle A quickly and the driver in vehicle C is also warned by the same information although he cannot see vehicle A. In the second scenario, vehicle A sends an emergent break message. The driver who has received this event can respond in time so as to avoid potential collision despite the obstructed view.

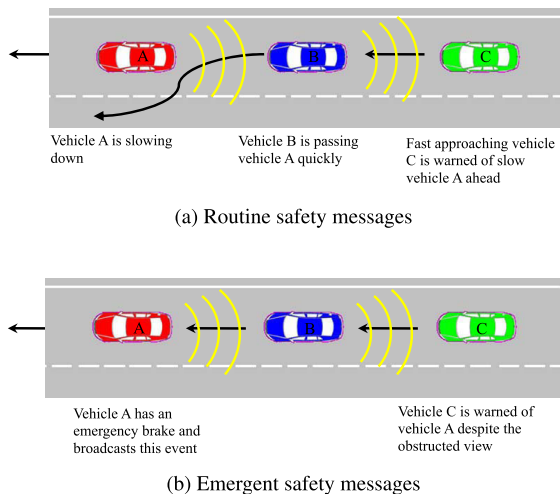


FIGURE 3. Two types of the safety messages.

#### IV. ANALYTICAL MODEL

The analytical model for IEEE 802.11p EDCA in the highway broadcast environment is introduced in this section. It is assumed that an ideal channel without bit error can be caused by channel fading, yet the impact of hidden terminals on vehicular networks is considered. In addition, both the saturated and unsaturated condition are considered.

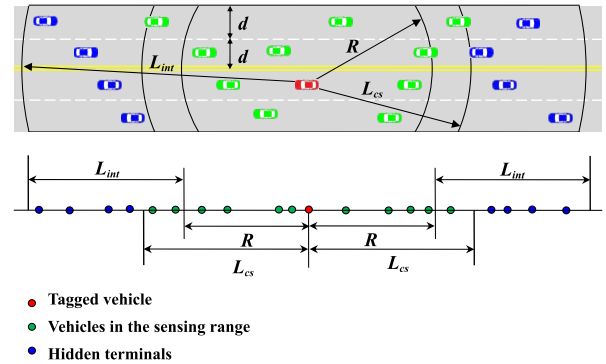


FIGURE 4. Two-dimensional VANET model.

More details of our study scenario are described in the below subsection.

#### A. HIGHWAY MODEL

According to Figure 4, a 2-D VANET model of a bidirectional highway with  $k$ -lane in every direction is shown in this paper. The distance between two parallel lanes is  $d$ . According to the empirical data, it is proved that an exponential distribution gears to the traffic of highway vehicle regarding the inter-vehicle distance and that the vehicles are spread in a lane following the process of Poisson point process [23]. A homogeneous 2-D Poisson point process of intensity  $\beta$ , namely, the traffic density, is considered in this paper. Hence, the probabilities of finding  $n$  vehicles within an area  $A \subset \mathbb{R}^2$  is given as

$$P(n, A) = \frac{(\beta\mu(A))^n}{n!} e^{-\beta\mu(A)}, \quad (2)$$

where  $\mu(A)$  is the standard Lebesgue measure of  $A$  and  $R$  represents the field of real numbers. Let  $r_i$  denote the Euclidean distance to the tagged node from node  $i$ . The proof [24] shows that the 2D Poisson point process with intensity  $\beta$  can be changed to the 1-D process with intensity  $\beta\pi$ , which means  $r_i^2$  follows a 1-D Poisson process of intensity  $\beta\pi$  in our highway model.

As shown in Figure 4, the transmission range can be denoted by  $R$  as the distance of receiving or sending a packet successfully. It relies on the channel fading and the power of transmission. It is considered that in the model, the transmission range is far greater than the inter-lane distance. The carrier sensing range can be denoted by  $L_{cs}$  as the distance of sensing a signal and it is the vital parameter in the scheme of CSMA/CA. Unlike the current work, in the interference range of a certain node denoted by  $L_{int}$ , the transmissions of other nodes will cause packet loss to the node. As shown by the measurement researches in [25], in terms of the above-mentioned three ranges, the relationship is:  $R \leq L_{int} \leq L_{cs}$ . Figure 4 indicates that the blue nodes are hidden terminals out of the carrier sensing range yet can interfere the nodes in the tagged node’s transmission range.

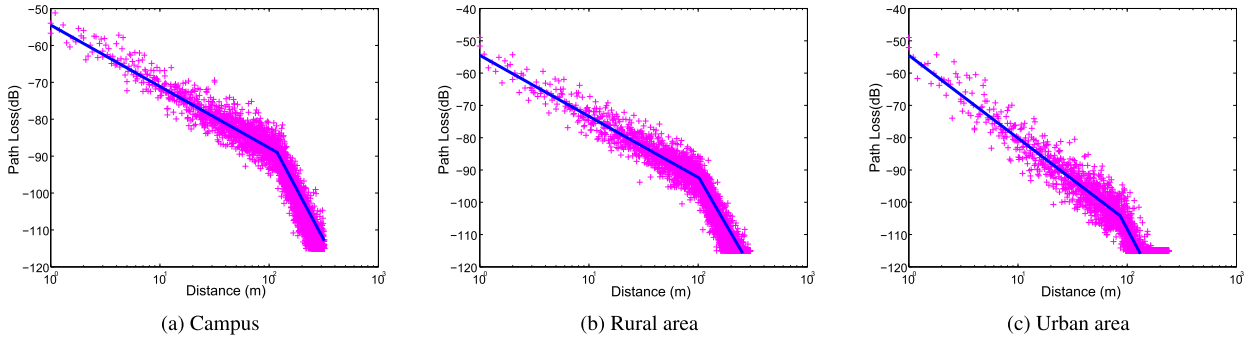


FIGURE 5. Measurements and fitting of the dual-slope path loss model.

The scenarios for the broadcast of IEEE 802.11p on the mode of CCH continuous access are assumed as below:

- Two kinds of safety applications are modeled in a vehicle, including the application of routine safety (AC1) with lower priority and the application of emergent safety (AC0) with higher priority.
- Hundreds of bytes are long enough for a safety message, thus, it is usually sent in a single packet. It is assumed that the average packet size  $E[P]$  is the same for all the ACs.
- The same as the assumptions made in many studies [26], [27],  $\lambda_i$  as the packet arrival rate for each AC $i$  queue instance is the process of satisfied Poisson distribution regarding the packets per second.
- In the time of transmitting message, vehicle mobility has been neglected since the nodes are almost stationary. The results of the paper show that the vehicles at the speed of 120 mi/h just move around 0.053m in the packet transmission period. Thus, the probability of link breaking is estimated as 0.0052 [28].

**B. PROPAGATION MODEL AND PHY-LAYER MODEL**

As shown in [29], having been completely characterized and evaluated in the realistic environment of the highway at the band of 5.9 GHZ, a model of the mathematical channel is utilized. Because of the obstruction by the huge obstacles between the receiver and the transmitter, the model simulates the attenuation of monotonic signal power with distance as well as describes the variation of signal power.

The model consists of a log-normal shadowing model ( $P_s$ ) and a dual-slope piecewise linear path loss model ( $P_p(d)$ ). And the signal power received refers to the function of distance  $d$  which can be shown as below:

$$\begin{aligned}
 P_r(d) &= P_p(d) + P_s \\
 &= \begin{cases} P(d_0) - 10\gamma_1 \log_{10}(d/d_0) + X_{\sigma_1}, & d_0 \leq d \leq d_c \\ P(d_0) - 10\gamma_1 \log_{10}(d_c/d_0) - 10\gamma_2 \log_{10}(d/d_c) \\ + X_{\sigma_2}, & d > d_c, \end{cases}
 \end{aligned}
 \tag{3}$$

where  $P(d_0)$  denotes the strength of signal as calculated with the usage of the model of free space path loss at the

reference distance  $d_0$ .  $d_c$  means the critical distance.  $\gamma_1$  and  $\gamma_2$  refer to the exponents of path loss.  $X_{\sigma_1}$  and  $X_{\sigma_2}$  denote the random, zero-mean variables respectively distributed with the standard deviations  $\sigma_1$  and  $\sigma_2$  respectively.

Three data sets obtained from the measurements in urban area, rural area and campus are provided in Figure 5. These data include the path loss and the corresponding distance between the receiver and the sender. The linear regression on the data sets as measured can be utilized to obtain the parameters of the dual-slope piecewise linear model [30]. Table 2 indicates the result.

TABLE 2. Fit parameters of the empirical model.

Parameter	Value		
	Campus	Rural area	Urban area
$d_0$	1m	1m	1m
$d_c$	218m	182m	102m
$\gamma_1$	1.66	1.89	2.56
$\gamma_2$	5.53	5.86	6.34
$X_{\sigma_1}$	2.8dB	3.1dB	3.9dB
$X_{\sigma_2}$	3.2dB	3.6dB	5.2dB

The technique of OFDM, dividing the total bandwidth to sixty-four sub-carriers, is used by IEEE 802.11p PHY-layer. And three coding rates and four modulation types are further defined in the protocol of 802.11p. The bit rates as perceived are decided by the coding rates and modulation utilized in transmissions. Here two definitions are provided.

*Definition 1 (SINR Threshold):* A node can successfully decode a packet only if the SINR of this packet at receiver is larger than the SINR threshold (denoted by  $S_{th}$ ).

*Definition 2 (Carrier Sensing Threshold):* A node can sense the transmitter only when the received signal strength is larger than the carrier sensing threshold (denoted by  $C_{th}$ ).  $C_{th}$  of the DSRC radio used in our experiment is  $-99$ dBm.

Table 3 gives the defined transmissions options and the corresponding  $S_{th}$  in IEEE 802.11p.

The carrier sensing range and the average transmission range as below can be calculated according to the given

TABLE 3. Bit rates in IEEE 802.11p.

Modulation	Coding rate	Bit Rate (Mbps)	SINR Threshold (dB)
BPSK	1/2	3	5.1
BPSK	3/4	4.5	6.5
QPSK	1/2	6	8.4
QPSK	3/4	9	12.3
16QAM	1/2	12	15.9
16QAM	3/4	18	20.2
64QAM	1/2	24	25.3
64QAM	2/3	27	32.6

thresholds and the channel fading model.

$$R = \begin{cases} E[d_0 10^{\frac{P_r(d_0) - S_{th} - W_N + X_{\sigma 1}}{10\gamma_1}}], & d_0 \leq R \leq d_c \\ E[d_c 10^{\frac{P_r(d_0) - 10\gamma_1 \log_{10}(d_c/d_0) - S_{th} - W_N + X_{\sigma 2}}{10\gamma_2}}], & R > d_c, \end{cases} \quad (4)$$

$$L_{cs} = \begin{cases} E[d_0 10^{\frac{P_r(d_0) - C_{th} + X_{\sigma 1}}{10\gamma_1}}], & d_0 \leq L_{cs} \leq d_c \\ E[d_c 10^{\frac{P_r(d_0) - 10\gamma_1 \log_{10}(d_c/d_0) - C_{th} + X_{\sigma 2}}{10\gamma_2}}], & L_{cs} > d_c, \end{cases} \quad (5)$$

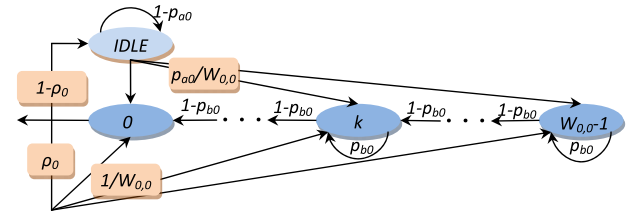
where  $W_N$  refers to the thermal noise.  $S_{th}$ ,  $C_{th}$  and  $W_N$  are radio-dependent constant values. We assume identical devices that all these values are the same for all radios.

Finally, we can utilize the traffic density  $\beta$ , to generate the average amount of vehicles respectively in the hidden terminal field, carrier sensing range and transmission range.

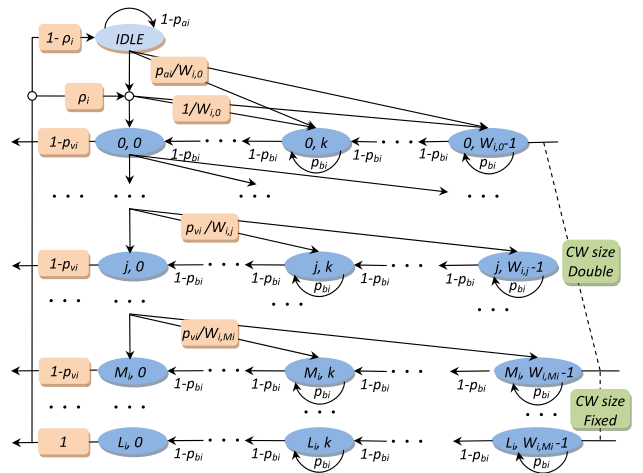
$$\begin{cases} N_{tr} = 2\beta\mu(R) \\ N_{cs} = 2\beta\mu(L_{cs}) \\ N_{ht} = 2\beta\mu(R + L_{int} - L_{cs}) \\ \mu(x) = \frac{\pi x^2 (\arccos(x - kd)/x) / 180 - (x - kd) x \sqrt{(2(kdx - k^2 d^2))/x^2}}{180} \end{cases} \quad (6)$$

C. BACKOFF MECHANISM MODELING FOR 802.11P EDCA BROADCAST

Each AC in a single node has the independent backoff instance if no virtual collision occurs [31]. The source node cannot know whether the transmission succeeds or not as there exists no frame of ACK in the broadcast mode. Hence, the procedure of backoff can be simplified as a single-dimensional Markov chain like Ma's model and no retransmission will be stimulated [6]. However, because of multiple ACs with various priorities in a node, different backoff instances are not completely independently. Virtual collision takes place if two or more ACs attempt to transmit. Other lower priority ACs should start a new stage of backoff with double CW in this case while the highest priority AC will access channel successfully. Hence, in our backoff mechanism modeling, there are two Markov chains as shown in Figure 6. The one-dimensional chain is for the AC of high priority emergent safety messages, and the two-dimensional chain is for the AC of low priority routine safety messages.



(a) One-dimensional Markov chain for higher priority AC0



(b) Two-dimensional Markov chain for lower priority AC1

FIGURE 6. Markov chain model for backoff instance.

The virtual collision is calculated by the external and internal transmission probabilities which is given as

$$\begin{cases} p_{v0} = 0 \\ p_{v1} = \varpi_0 \\ \tau_0 = \varpi_0 \\ \tau_1 = \varpi_1(1 - p_{v1}) = \varpi_1(1 - \varpi_0) \end{cases} \quad (7)$$

where,  $\varpi_i$  refers to the internal transmission probability that the AC[i] tries to send the packet observed by other ACs in the same node. The external transmission probability of (denoted by  $\tau_i$ ) which means the transmission observed by other nodes in the sensing range of a node can be expressed by the virtual collision probability and the internal transmission probability.

The total of all the external transmission probabilities of ACs within this node is the total transmission probability of one node. Here, the definitions of probabilities that have been used are offered in the Markov Chain model [32].

Definition 3 (Packet Arrival Probability): The probability that it has packets arrival in a virtual slot. The below formula can calculate the probability with packets at every queue of MAC in a virtual slot since the distribution of Poisson is followed by the emergent safety message (AC0)'s packet arrival rate and the routine safety message (AC1) is

generated periodically.

$$\begin{cases} p_{a0} = \sum_{k=1}^{\infty} \frac{(\lambda_1 v_{\sigma})^k}{k!} e^{-\lambda_1 v_{\sigma}} = 1 - e^{-\lambda_1 v_{\sigma}} \\ p_{a1} = \lambda_0 v_{\sigma} \end{cases} \quad (8)$$

where the virtual slot denotes the time interval between the two backoff counter decrements of stations without transmission. This discrete time scale is not the system time slot  $\sigma$  since the backoff procedure will be frozen when the channel is busy. Hence, the virtual slot is commonly much longer than the slot time  $\sigma$  which is given as

$$v_{\sigma} = (1 - p_{bi})\sigma + p_{bi}T_{bi} \quad (9)$$

In equation 9,  $T_{bi}$  is the average blocking time of AC $i$ . If the backoff procedure of AC $i$  is frozen, it will keep current state for a period of a packet transmission time and an AIFS[ $i$ ].

*Definition 4 (Backoff Blocking Probability):*  $p_{bi}$  equals the probability that the node can sense other nodes occupying the channel or there exists a transmission attempted by other ACs in the node for a particular backoff instance of AC within a node. The probability of backoff blocking is calculated by the formula as below as the ACs with lower priority are deferred for a longer time than the ACs with higher priority and AIFSN is bigger.

$$p_{bi} = 1 - \left[ P(k) \prod_{\substack{j=0 \\ j \neq i}}^{A_i+1} (1 - \tau_j) \right], \quad i = 0, 1$$

$$P(k) = \sum_{k=0}^{\infty} (1 - \tau)^{N_{cs}-1} \frac{(N_{cs} - 1)^k}{k!} e^{-(N_{cs}-1)} \quad (10)$$

*Definition 5 (Non-Empty Queue Probability):* Stands for the probability that one packet is waiting in the AC $i$  queue. That is, the usage of the server for AC $i$ 's MAC queue can be defined as:

$$\rho_i = \frac{\lambda_i}{\mu_i}, \quad i = 0, 1 \quad (11)$$

where  $\mu_i$  denotes the queue's average service ratio in packets per second. On the one side, there is no packet to send in the extreme non-saturated case if  $\rho_i = 0$  can be satisfied. On the other side, the status of IDLE will be removed from the Markov Chain when  $\rho_i$  equals 1. Thus, the model changes  $\rho_i$  from 0 to 1 to cover the extreme saturated, intermediate non-saturated and non-saturated conditions.

Based on the above probabilities, following the similar procedure to solve two Markov chains, we have

$$\begin{cases} \omega_0 = b_{0,0} = \left[ \frac{(W_{0,0} + 1)}{2(1 - p_{b0})} + \frac{1 - \rho_0}{p_{a0}} \right]^{-1} \\ \omega_1 = \sum_{j=0}^L b_{1,j,0} = \frac{1 - p_{v1}^{L+1}}{1 - p_{v1}} b_{1,0,0} \end{cases} \quad (12)$$

where  $b_{1,j,k}$  represents the stationary probabilities of state  $j, k$  in two-dimensional Markov chain (backoff stage is  $j$ , backoff counter is  $k$ ).

#### D. MAC ACCESS DELAY ANALYSIS

The deviation, mean and distribution of the MAC access delay are derived in the subsection. When a packet is the MAC queue's head to the time instant that the packet can be received successfully, the MAC access delay can be defined as the duration from the time instant. In many literatures, the MAC access delay is referred to as the MAC service time when the wireless node is modeled as a queuing system. When the time is divided by a small unit ( $\{q_{i,k}\}$  refers to the probability in a stable state that the time of packet service is equal to  $\{ts_{i,k}\}$  slottime), it is a non-negative random variable of which the distribution can be considered as a discrete time sequence  $\{ts_{i,k}\}$  with the probability  $\{q_{i,k}\}$ . The PGF of the MAC access delay ( $T_{Si}$ ) is given by

$$P_{T_{Si}}(z) = \sum_{k=0}^{\infty} q_{i,k} z^{ts_{i,k}} \quad (13)$$

Let  $TR(z)$  be the PGF of the transmission time. One packet transmission time is a constant value ( $T_{tr}$ ), the PGF is as below assuming that all the messages about safety have the same length of packet.

$$TR(z) = z^{T_{tr}} \quad (14)$$

Let  $H_i(z)$  be the average time's PGF that the backoff counter reduces by one of AC $i$ . It will be blocked for the  $T_{tr} + AIFS[i]$  period when another transmission can be identified. The reason for that is the backoff counter of AC $i$  decreases by each slot time ( $\sigma$ ) once the channel is idle. This PGF is given as

$$H_i(z) = (1 - p_{bi})z^{\sigma} + p_{bi}z^{T_{tr}+AIFS[i]}, \quad i = 0, 1. \quad (15)$$

Let  $B_i(z)$  be the average time's PGF that the backoff counter decreases from the initial window size to 0. We can obtain  $B_i(z)$  by using mason formula if the whole EDCA backoff procedure is deemed as the linear system of Z-transform domain.

$$\begin{cases} B_{0,0}(z) = \frac{1}{W_{0,0}} \sum_{k=0}^{W_{0,0}-1} [H_0(z)]^k \\ B_{1,j}(z) = \begin{cases} \frac{1}{W_{1,j}} \sum_{k=0}^{W_{1,j}-1} [H_1(z)]^k, & j \in (1, M_1) \\ \frac{1}{W_{1,M_1}} \sum_{k=0}^{W_{1,M_1}-1} [H_1(z)]^k, & j \in (M_1, L) \end{cases} \end{cases} \quad (16)$$

Finally, similar to get  $B_i(z)$ , we also can solve the PGF of  $P_{T_{Si}}$  by using mason formula.

$$\begin{cases} P_{T_{S0}}(z) = TR(z)B_0(z) = \frac{TR(z)}{W_{0,0}} \sum_{k=0}^{W_{0,0}-1} [H_0(z)]^k \\ P_{T_{S1}}(z) = (1 - p_{v1}) TR(z) \sum_{n=0}^L \left[ p_{v1}^n \prod_{j=0}^n B_{1,j}(z) \right] \\ \quad + p_{v1}^{L+1} \prod_{j=0}^L B_{1,j}(z) \end{cases} \quad (17)$$



The definition of PGF shows that the deviation and mean of the MAC access delay can be obtained.

$$T_{Si} = \frac{1}{\mu_i} = \frac{dP_{Tsi}(z)}{dz} \Big|_{z=1} = P_{Tsi}'(1), \quad i = 0, 1. \quad (18)$$

$$D_{Si} = P_{Tsi}''(1) + P_{Tsi}'(1) - [P_{Tsi}'(1)]^2, \quad i = 0, 1. \quad (19)$$

To solve the multivariate nonlinear equations composed of (7), (8), (10) and (12) with 10 variables  $\rho_i, p_{vi}, p_{bi}, \varpi_i$  and  $\tau_i$  ( $i = 0, 1$ ), we first initialize  $\rho_i$  according to the network condition, and then use the iterative method to obtain other 8 variables. Iteration can be completed when all  $\rho_i \leq \varepsilon$  can be satisfied, in which  $\varepsilon$  refers to an error bound which has been previously defined.

Finally, based on PGF's properties, the probability density function (PDF) of the MAC access delay can be derived.

$$p_k(t_{si}) = P\{t_{si} = k\} = \frac{P_{Tsi}^{(k)}(0)}{k!}, \quad i = 0, 1 \quad (20)$$

## V. MODEL VALIDATION

### A. SIMULATION

In this section, we first compare the theoretical values of our model for the mean, standard deviation, and PDF of the MAC access delay with simulation results using NS2 simulator. The packet size of 100 bytes is normally long enough to show the vehicles' basic status. Nonetheless, the length should be longer in consideration of safety. The packet size  $E[P]$  is set to be 500 bytes in this paper. Every vehicle has two active ACs with the packet arrival ratios of 10pkts/s (AC1) and 2pkts/s (AC0). A moderate value 500m is chosen as the transmission range  $R$  at the rate of 6Mbps in simulation as the transmission range of IEEE 802.11p reaches 1000m at the data ratio of 3Mbps and less than 200m at the data ratio of 27Mbps. Table 4 stands for IEEE 802.11p's network parameters and the traffic parameters of a regular highway environment.

TABLE 4. Traffic and network parameter settings.

Parameter	Value	Parameter	Value
Highway length	2200m	PHY header	48bits
Density	0.01~0.1 vhls/m	MAC header	112bits
Average distance	100m~10m	Date rate	3Mbps
Transmission range	500m	Basic rate	1Mbps
Carrier sensing range	700m	Slot time	13μs
Interference range	600m	SIFS	32μs
Retry limit	4	Propagation delay	2μs

The mean access delay and standard deviation of IEEE 802.11p MAC layer with the changing density of traffic are respectively indicated in Figure 7 and Figure 8. It is shown that the simulating results and analytical values have a sound agreement. It can be observed that ACs with lower and higher priority have low average delay of access. Nonetheless, AC1's standard deviation curve quickly increases the density of traffic. It is shown that the maximal delay can largely deviate from the average delay. Thus, the real condition of

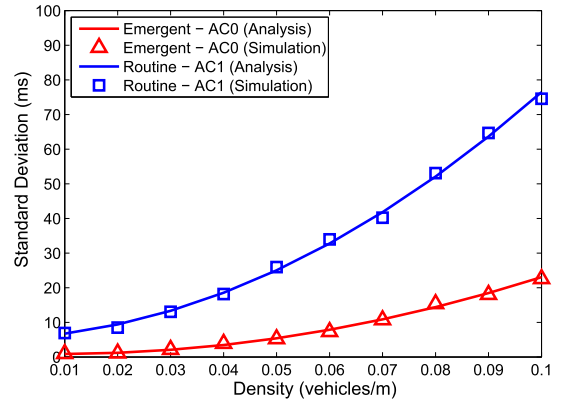


FIGURE 7. Mean of the MAC access delay.

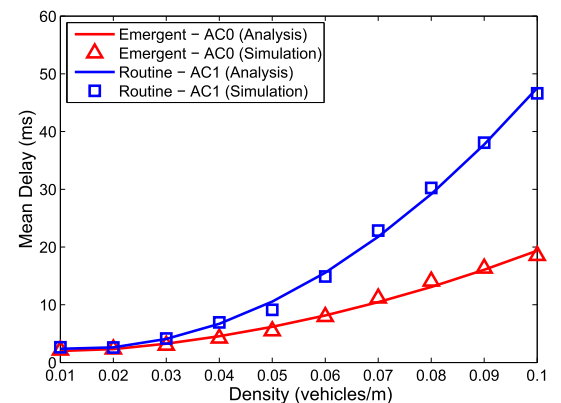


FIGURE 8. Standard deviation of the MAC access delay.

network cannot be shown by the mean value at heavy density of traffic. At the traffic density (0.1 vhls/m), the maximal delay of AC1 in the simulation is more than 300ms.

The probability distribution of MAC access delay with the changing density of traffic is indicated in Figure 9. It can be observed that all the results from analysis can well match the simulating results. And the model has the tail distribution with the simulations.

### B. EXPERIMENT

This section further validates our model in a real-world testbed composed of DSRC radios. The experimental device is an IEEE 802.11p compliant radio (IWCU OBU4.2) with a GPS module and a 5.9GHz antenna. According to a 32 bits MIPS processor (Atheros AR7130) at 300MHz, it is in the Linux machine (kernel 2.6.32). Each IWCUOBU4.2 connects to a laptop through the interface of Ethernet to record timestamps of sent or received packets. The testbed is composed of 20 IWCU OBU4.2 devices. The experiment is conducted in the campus environment as shown in Figure 10. Table 5 shows the basic settings of communication parameters. The red point is the tagged node. We analyze the packet delay distribution of this node.

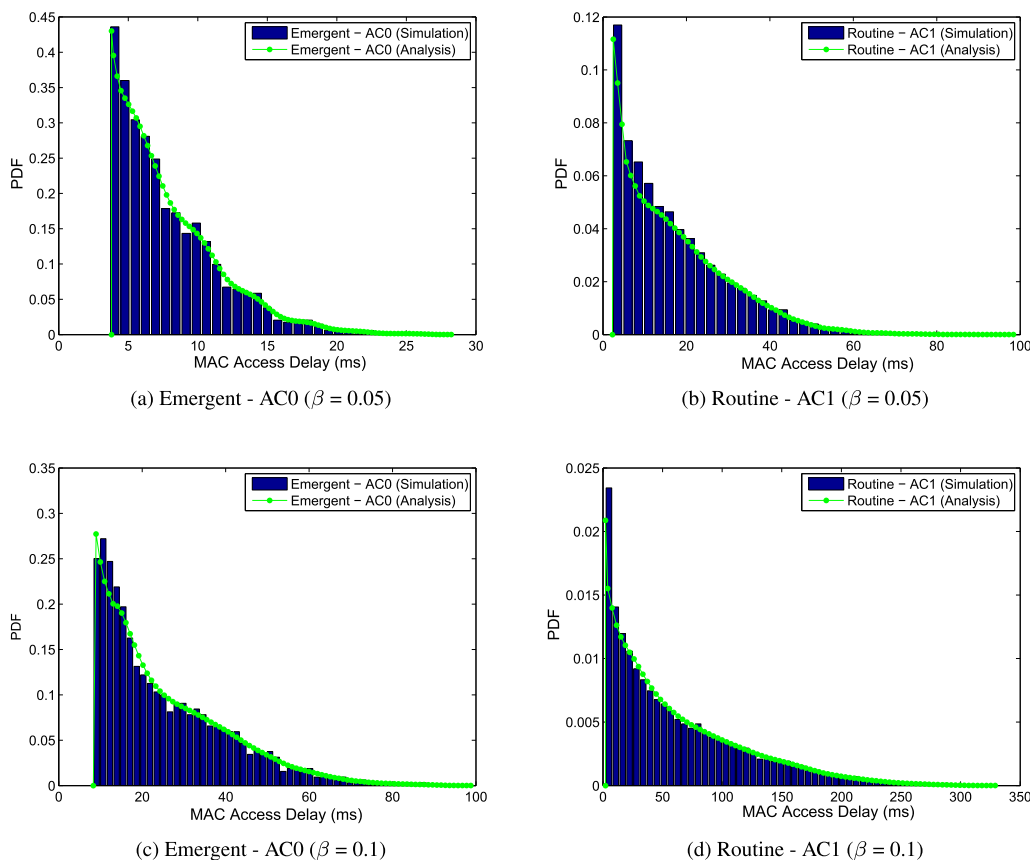


FIGURE 9. PDF of the MAC access delay (Simulation results).

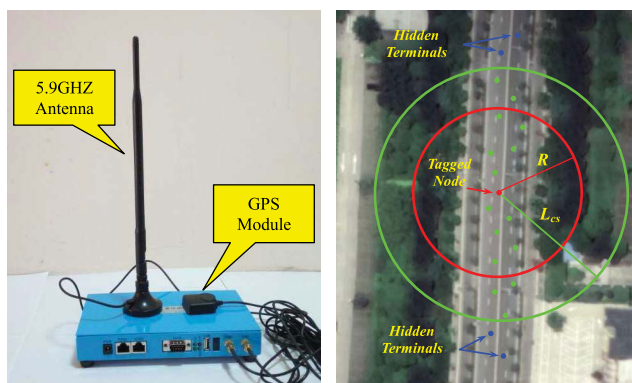


FIGURE 10. Experiment setup.

TABLE 5. Basic parameter settings.

Parameter	Value
Transmission power	20dBm (EIRP)
RX sensitivity	-95 dBm
Center carrier frequency	5.890MHz (Control Channel)
Channel width	10MHz
Data rate	6Mbps
Packet size	500Bytes

The probability distribution of MAC access delay is shown in Figure 11. The experimental results well match the results from analyses.

## VI. NUMERICAL ANALYSIS

### A. THE IMPACT OF CARRIER SENSING THRESHOLD ON MAC ACCESS DELAY

We first analyze the impact of Carrier Sensing Threshold on MAC Access Delay. The traffic density is  $0.05\text{vhls}/\text{m}$  and the Carrier Sensing Threshold is changing from  $600 \sim 1000\text{m}$ . As shown in Figure 12, the mean of the MAC access delay decreases with increasing Carrier Sensing Threshold.

If the Carrier Sensing Threshold gets larger and the interference threshold remains constant, the range of hidden terminals will get smaller accordingly. That means the number of hidden terminals ( $N_{cs}$ ) is decreasing. With decreasing  $N_{cs}$  the backoff blocking probability is getting smaller based on Eq. 10. The virtual slot ( $v_\sigma$ ) is also reduced according to Eq. 9 since  $T_{bi}$  is much greater than  $\sigma$ . Therefore, the collision probability will decrease which greatly reduces the packet losses and retransmissions. Finally, it largely shortens the mean access delay.

### B. HYPOTHESIS TEST FOR MAC ACCESS DELAY DISTRIBUTION

AC $_i$  will obtain a minimal delay value as noted by  $a_i$  in the work if an AC $_i$  detects that the channel is idle for AIFS[ $i$ ] and can access the channel without contention. The minimal delay as below can be easily obtained with the data ratio and

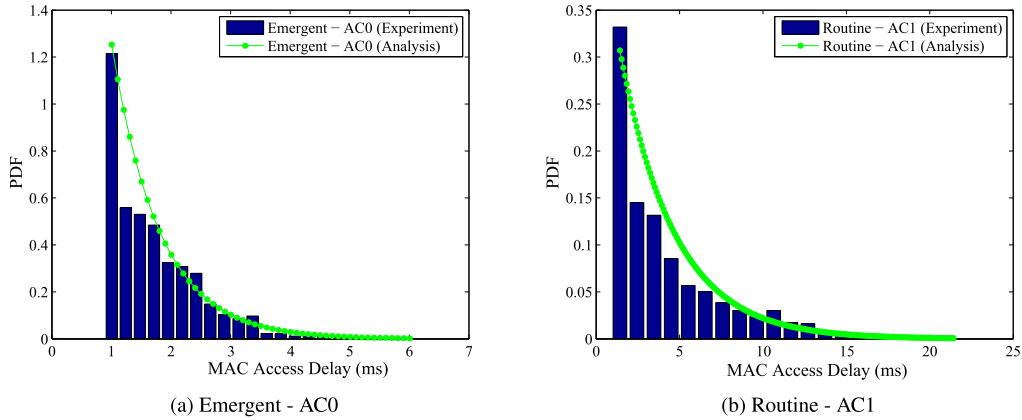


FIGURE 11. PDF of the MAC access delay (Experiment results).

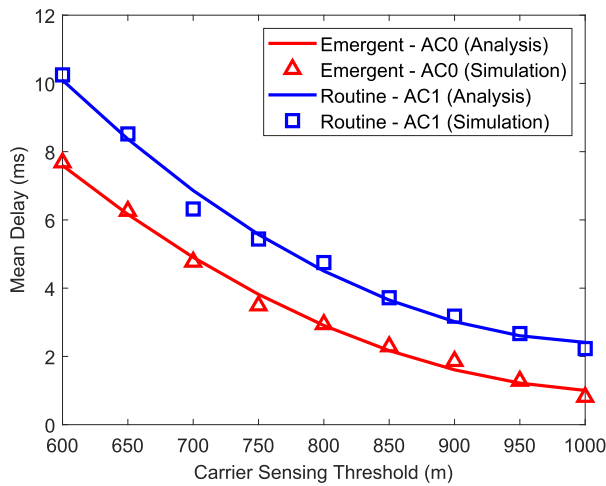


FIGURE 12. Mean of the MAC access delay vs.  $C_{th}$ .

the size of the particular packet.

$$a_i = AIFS[i] + T_{tr}, \quad i = 0, 1 \quad (21)$$

In our simulation,  $a_0$  and  $a_1$  are 1.5371 ms and 1.5631 ms, respectively. Therefore, we assume the distribution of MAC access delay of AC $i$  is the same as an exponential distribution with PDF defined as follows

$$f_i(x) = \begin{cases} \theta_i e^{-\theta_i(x-a_i)}, & x \geq a_i \\ 0, & x < a_i \end{cases}, \quad i = 0, 1 \quad (22)$$

The PDF properties show that the deviation, mean and cumulative distribution function (CDF) can be further derived.

$$E[X_i] = \int_{a_i}^{\infty} x f_i(x) dx = \frac{1}{\theta_i} + a_i, \quad i = 0, 1 \quad (23)$$

$$E[X_i^2] = \int_{a_i}^{\infty} x^2 f_i(x) dx = \frac{2}{\theta_i^2} + \frac{2a_i}{\theta_i} + a_i^2, \quad i = 0, 1 \quad (24)$$

$$D[X_i] = E[X_i^2] - E^2[X_i] = \frac{1}{\theta_i^2}, \quad i = 0, 1 \quad (25)$$

$$F_i(x) = \begin{cases} 1 - e^{-\theta_i(x-a_i)}, & x \geq a_i \\ 0, & x < a_i \end{cases}, \quad i = 0, 1 \quad (26)$$

Kolmogorov-Smirnov (K-S) Test [33] is used in this paper for the analysis of MAC access delay distribution. The K-S test considers the distance between the cumulative distribution function of the reference distribution and empirical distribution function of the sample.

Given a sample of  $n$  observations, let  $S_n(x)$  be the empirical distribution function of sample. According to the cumulative distribution function denoted by  $F(x)$  of a reference distribution, thus, the distance  $D_n$  is calculated by

$$D_n = \max_x |S_n(x) - F(x)| \quad (27)$$

If  $D_n > C_\alpha$  is satisfied, then the hypothesis is reject at significance level  $\alpha$ , where  $P\{x \leq K_\alpha\} = 1 - \alpha$  and  $C_\alpha = \frac{K_\alpha}{\sqrt{n}}$  is called critical value.

In this section, we will test two samples. One is derived from simulation, and the other is generated with PDF of our analytical model. The steps of hypothesis test are listed below.

First, we state null hypothesis and alternative hypothesis.

$H_0$ : The distribution of access delay follows the exponential distribution

$H_1$ : The distribution of access delay does not follow the exponential distribution

Then, we calculate the maximum likelihood estimate (MLE) of the parameter of the reference exponential distribution by

$$\frac{1}{\hat{\theta}_i} = \bar{X}_i - a_i, \quad i = 0, 1 \quad (28)$$

where  $\bar{X}_i$  is the mean of  $n_i$  samples of MAC access delay of AC $i$ .

Finally, we compare the maximum distance  $D_{ni}$  to the critical value at significance level  $\alpha$ . The results are shown in Figure 13 and Table 6.

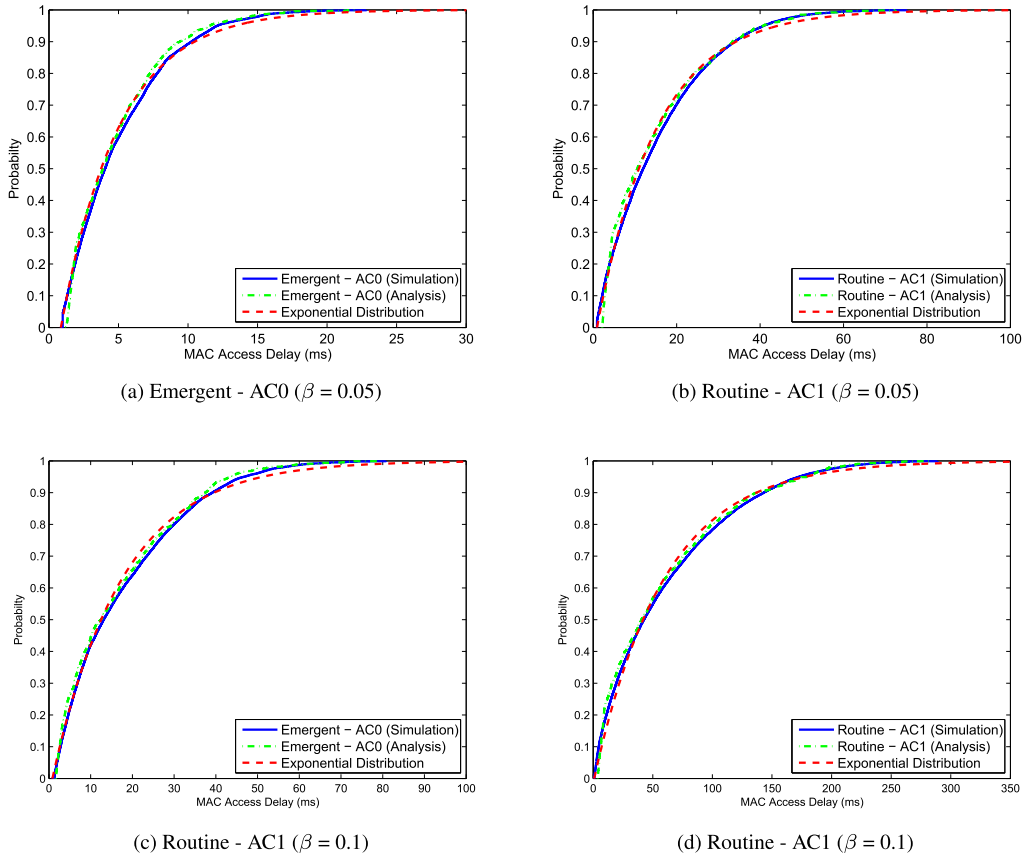


FIGURE 13. CDF of the MAC access delay.

TABLE 6. Results of K-S test.

Density	$D_{n0}/D_{n1}$ (Simulation)	$D_{n0}/D_{n1}$ (Analysis)	Conclusion
0.01	0.2510/0.2076	0.1672/0.1378	reject $H_0$
0.02	0.1272/0.0945	0.1111/0.0821	reject $H_0$
0.03	0.0425/0.0418	0.0401/0.0387	accept $H_0$
0.04	0.0352/0.0351	0.0307/0.0321	accept $H_0$
0.05	0.0335/0.0394	0.0253/0.0374	accept $H_0$
0.06	0.0334/0.0368	0.0278/0.0327	accept $H_0$
0.07	0.0325/0.0321	0.0299/0.0318	accept $H_0$
0.08	0.0348/0.0339	0.0245/0.0324	accept $H_0$
0.09	0.0392/0.0387	0.0376/0.0349	accept $H_0$
0.10	0.0421/0.0413	0.0406/0.0392	accept $H_0$

We choose sample size 1000 and  $\alpha = 0.05$ . Hence, the critical value  $C_\alpha$  is derived as 0.0430 by standard table look-up for K-S test [34]. Compared with the maximum distance  $D_{ni}$  in Table 6, we found that the hypothesis passes the test in the case of jammed traffic, while it fails the test when the traffic is smooth. However, the exponential distribution also seems to be a rational approximation to the distribution of MAC access delay.

We can use the approximation to simplify the analytical model of the distribution of MAC access delay. For the

particular parameters of highway traffic and the parameters of predesigned network, it is easy to calculate the minimum delay ( $d_{min}$ ) and mean access delay ( $d_{mean}$ ) by equations (18) and (21). Obviously, these two values can make a good estimation to the parameter  $\theta$  with the following formula:

$$\hat{\theta} = \frac{1}{d_{mean} - d_{min}} \tag{29}$$

C. DEADLINE MISS RATE

Although the delay limitation is more than the mean delay, a safety application may not meet the real-time requirement because of IEEE 802.11p stochasticity of protocol. Furthermore, it is difficult to determine whether a safety message can be received successfully before deadline. Thus, the Deadline Miss Rate denoted by  $DMR_i$  for every  $AC_i$  is introduced to assess whether the real-time requirement can be satisfied by a safety application. As for the particular delay constraint  $D_c$ , based on the Complementary Cumulative Distribution Function (CCDF) of the approximated exponential distribution,  $DMR_i$  can be derived.

$$\begin{aligned} DMR_i &= \bar{F}_i(D_c) = 1 - F_i(D_c) \\ &= e^{-\hat{\theta}(D_c - a_i)}, \quad i = 0, 1. \end{aligned} \tag{30}$$

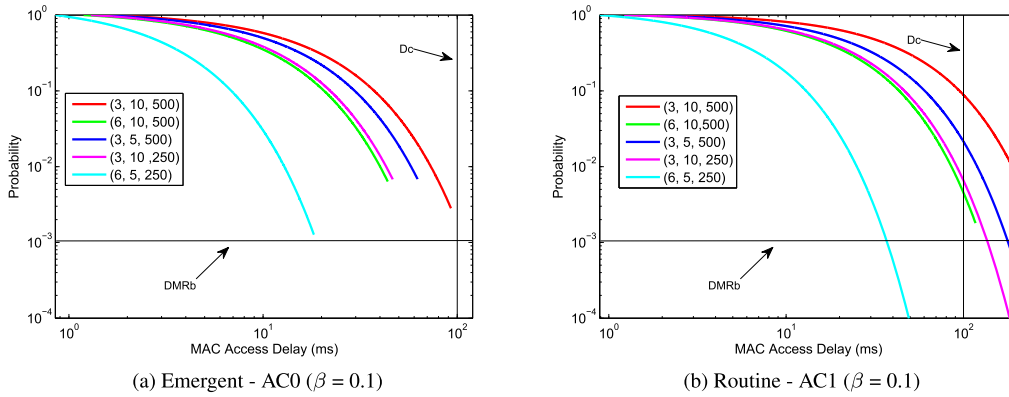


FIGURE 14. CCDF of the MAC access delay.

According to [35], an allowable maximal delay requirement for safety applications which have been commonly utilized (for instance, the warning of intersection collision and the warning of forward collision) is 100 ms. Denoted by  $DMR_b$ , Deadline Miss Rate Bound is set as  $10^3$  in this paper. It suggests that the deadline is missed by one out of one thousand packets. The targets of performance assess the influences of various parameters of network on the MAC access delay. The CCDF curves of MAC access delay are shown in Figure 14. Every curve is parameterized by the triplet (packet size [Bytes], bit rate [Mbps] and packet arrival rate [packets per second]). The data show that the higher-priority messages about emergent safety can meet the deadline. However, the lower-priority messages about routine safety cannot assure the real-time requirement in a majority of cases except for the smaller size of packet, the lower packet arrival ratio, and the higher bit ratio. In addition, if the size of packet and the packet arrival ratio are reduced and the bit rate is increased, it is possible to assure the real-time broadcast. Nonetheless, the ranges of the three parameters are somewhat limited in real practices. For instance, the delay can be greatly reduced by the higher bit ratio. Better channel quality is needed to interpret the higher coding rate packet and modulation correctly. Actually, in the environment of highway, the proper bit rate ranges from 3 to 6Mbps. The size of packet and the packet arrival ratio are more relative to the particular application.  $DMR_i$  can show an intuitive statistics value to the particular application with real-time requirement of the delay constraint  $D_c$ . Thus, for designers, it is a positive feedback to retune the parameters of network.

#### D. TAIL DISTRIBUTION ANALYSIS

The tail behavior of the delay distribution with the simplified model is studied in this section. For real-time applications, a key concern is whether the delay distribution has a heavy-tailed. With the definition of the heavy-tailed distribution, we obtain a negative conclusion.

*Proof:* Assuming that MAC access delay distribution has a heavy-tailed, by definition, we get following equation

$$\forall \gamma > 0, \lim_{x \rightarrow \infty} e^{\gamma x} \bar{F}(x) = \lim_{x \rightarrow \infty} e^{(\gamma - \theta)x + a\theta} = \infty \quad (31)$$

Then, we have

$$\forall \gamma > 0, \gamma > \theta. \quad (32)$$

Since  $\theta$  is a positive number, inequality (32) does not hold in all conditions. Therefore, the distribution of MAC access delay is not heavy-tailed distribution. ■

This result is just in contrast to the conclusion drawn by Taka Sakurai [36] studying the MAC delay distribution of IEEE 802.11 DCF unicast mode. A reasonable explanation of this difference is that in 802.11 DCF unicast, there are many control frames such as RTS, CTS and ACK. These handshaking schemes increase the transmission delay and the backoff blocking probability so as to prolong the total MAC access delay. Moreover, Taka Sakurai’s model is under saturated condition, however, the node in VANET is far from saturated status even in high traffic density. This conclusion indicates that broadcast mode is more suited for safety message transmission. In reality, IEEE 802.11p broadcast can be adopted to some applications with soft real-time requirement, but still need to be considered carefully when used in the critical real-time communications with mandatory deadline because of the unbounded delay characteristics.

#### E. QUEUING DELAY ANALYSIS

The MAC access delay distribution can be used to further analyze the queuing delay. The queuing delay is from the time when a packet arrivals in the queue to the time when it becomes queue’s head. Since we have proved that an exponential distribution (or approximates to an exponential distribution at lower traffic density) is followed by MAC access delay, the M/M/1/K model can be used to describe the MAC queue system with buffer size  $K$ .

As the packet arrivals satisfied Poisson process with rate  $\lambda_i$ , the probability denoted by  $\alpha_i(k)$  that  $k$  packets enter ACi’s

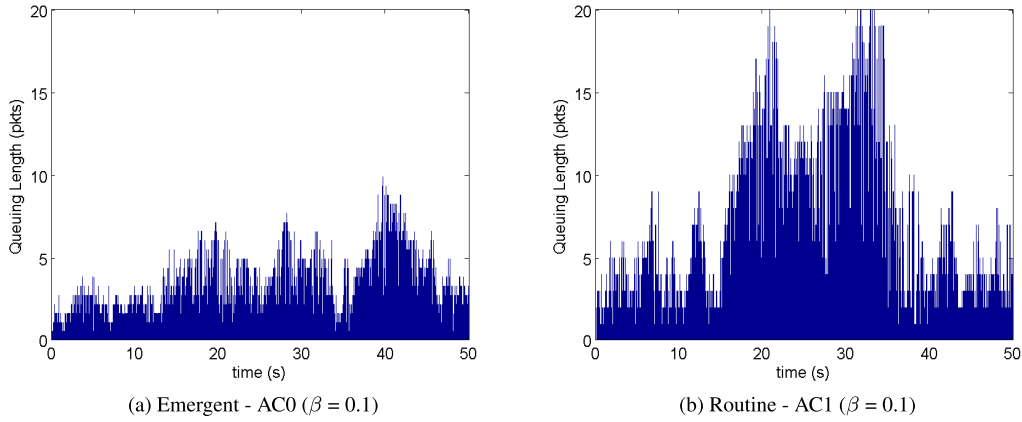


FIGURE 15. The change of the queue length (traffic density  $\beta = 0.1$  vhls/m).

queue during the MAC access time (service time) is as below:

$$\alpha_i(k) = \int_{t=0}^{\infty} \frac{(\lambda_i t)^k}{k!} e^{-\lambda_i t} P_{T_{S_i}}(t) dt \quad (33)$$

Let  $p_{i,j}$  ( $j = 1, 2 \dots K-1$ ) be the steady state probability that there are  $j-1$  packets waiting in the queue of AC $i$  and one is served. According to the balance equation, we have

$$\begin{cases} p_{i,0} = \frac{1 - \rho_i}{1 - \rho_i^{K+1}} \\ p_{i,j} = \rho_i^j \frac{1 - \rho_i}{1 - \rho_i^{K+1}} \end{cases}, \quad i = 0, 1; 1 \leq j \leq K \quad (34)$$

The average queue length, blocking probability and average queuing delay are given as

$$\begin{cases} L_i = \sum_{j=0}^{K-1} j p_{i,j+1} \\ p_{i,B} = p_{i,K} = \frac{(1 - \rho_i) \rho_i^K}{1 - \rho_i^{K+1}}, \quad i = 0, 1; 0 \leq j \leq K \\ T_{Wi} = \frac{L_i}{\lambda_i(1 - p_{i,B})} \end{cases} \quad (35)$$

Figure 15 shows the change of the queue length in a single simulation run at the traffic density of 0.1 vhls/m. Both queue lengths of different messages are very short, which indicates that the safety communication in VANET is under non-saturated condition although the traffic density is very high.

Figure 16 and Figure 17 show that the M/M/1/K model works well to predict the average queue length and the average queuing delay. Besides, average queuing delay indicates the similar tendency to the traffic density with the similar mean value and the MAC access delay. This is because both delays are dependent on the utilization of the queue and the blocking probabilities. If the backoff procedure is frozen by the busy channel, until the backoff counter is resumed,

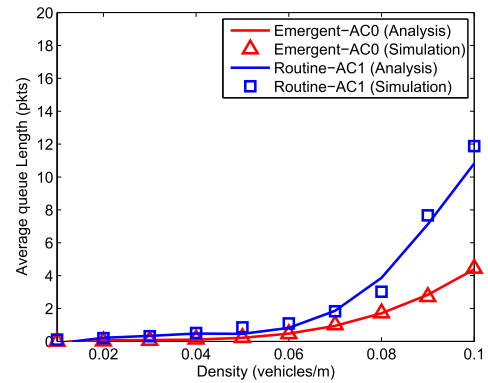


FIGURE 16. The average queue length.

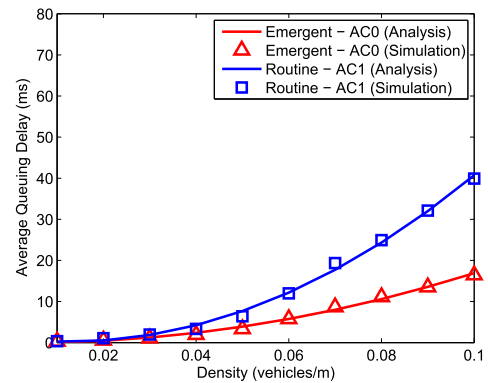


FIGURE 17. The average queuing delay.

the service of the queue system will also be blocked. Therefore, the probability of backoff blocking almost equals the probability of queue blocking.

## VII. CONCLUSION

The performance of the protocol of IEEE 802.11p MAC utilized in the communications of V2V safety with two priority messages in a regular environment of highway is assessed in this paper. We only consider the one-hop broadcast and the

continuous access mode. And in order to generate the explicit expressions of probability distribution, mean and deviation of MAC access delay, we propose an analytical model. The K-S test is adopted in this paper to prove that an exponential distribution is a sound approximation for the MAC access delay, particularly in the heavy traffic condition. Therefore, the analytical model can be simplified, and the queuing delay and tail distribution of the MAC layer can be further analyzed. In our future work, we will take the multi-hop broadcast and the other multi-channel access schemes into account.

There is no fixed upper bound on the access delay of IEEE 802.11p for a contention-oriented MAC scheme. A centralized node's demand will contradict the fast-changing and full-distributed vehicular network even though deterministic service can be provided by the conflict-free MAC approaches (TDMA, FDMA). As shown by analysis, the performance of higher priority class of traffic can be improved by the IEEE 802.11p EDCA for the support of QoS. However, lower priority ACs may still fail to meet the real-time requirement. We can utilize the MAC access delay distribution to obtain DMR with the statistical probability that the broadcast of message may exceed the deadline. This can help designers to adjust the parameters of network. Nonetheless, the real-time applications should be taken care of for the communications of V2V safety in the future due to the IEEE 802.11p MAC layer's non-determinism.

## REFERENCES

- [1] *Annual Performance Report Fiscal Year 2011*, U.S. Dept. Transp., Washington, DC, USA, 2011.
- [2] G. N. Wassim, K. Jonathan, D. S. John, and B. John, "Frequency of target crashes for intelligent safety systems," U.S. Dept. Transp. Nat. Highway Traffic Saf. Admin., Washington, DC, USA, Tech. Rep. DOT HS 811 381, 2010.
- [3] M. Nekoui and H. Pishro-Nik, "Analytic design of active vehicular safety systems in sparse traffic," in *Proc. 8th ACM Int. Workshop Veh. Inter-Netw.*, 2011, pp. 87–88.
- [4] G. Naik, B. Choudhury, and J.-M. Park, "IEEE 802.11bd & 5G NR V2X: Evolution of radio access technologies for V2X communications," *IEEE Access*, vol. 7, pp. 70169–70184, 2019.
- [5] A. Jafari, S. Al-Khayatt, and A. Dogman, "Performance evaluation of IEEE 802.11p for vehicular communication networks," in *Proc. 8th Int. Symp. Commun. Syst. Netw. Digit. Signal Process.*, Jul. 2012, pp. 1–5.
- [6] X. Ma, X. Chen, and H. H. Refai, "Performance and reliability of DSRC vehicular safety communication: A formal analysis," *EURASIP J. Wireless Commun. Netw.*, vol. 2009, no. 3, 2009, Art. no. 969164.
- [7] H. J. Qiu, I. W.-H. Ho, K. T. Chi, and Y. Xie, "A methodology for studying 802.11p VANET broadcasting performance with practical vehicle distribution," *IEEE Trans. Veh. Technol.*, vol. 64, no. 10, pp. 4756–4769, Sep. 2015.
- [8] G. Bianchi, "Performance analysis of the IEEE 802.11 distributed coordination function," *IEEE J. Sel. Areas Commun.*, vol. 18, no. 3, pp. 535–547, Mar. 2000.
- [9] F. Martelli, M. E. Renda, G. Resta, and P. Santi, "A measurement-based study of beaconing performance in IEEE 802.11p vehicular networks," in *Proc. IEEE INFOCOM*, Mar. 2012, pp. 1503–1511.
- [10] M. A. Salahuddin, A. Al-Fuqaha, and M. Guizani, "Exploiting context severity to achieve opportunistic service differentiation in vehicular ad hoc networks," *IEEE Trans. Veh. Technol.*, vol. 63, no. 6, pp. 2901–2915, Jul. 2014.
- [11] V. Kolici, T. Oda, E. Spaho, L. Barolli, M. Ikeda, and K. Uchida, "Performance evaluation of a VANET simulation system using NS-3 and SUMO," in *Proc. 29th Int. Conf. Adv. Inf. Netw. Appl. Workshops*, Mar. 2015, pp. 348–353.
- [12] N. Pramuanay, K. N. Nakorn, and K. Rojviboonchai, "Preliminary study of reliable broadcast protocol on 802.11p public transport testbed," in *Proc. IEEE ECTI-CON*, Jun. 2015, pp. 1–6.
- [13] Q. Wang, K. Jaffrs-Runser, J.-L. Scharbarg, C. Fraboul, Y. Sun, J. Li, and Z. Li, "A thorough analysis of the performance of delay distribution models for IEEE 802.11 DCF," *Ad Hoc Netw.*, vol. 24, no. B, pp. 21–33, Jan. 2015.
- [14] M. F. Uddin, "Throughput analysis of a CSMA based WLAN with successive interference cancellation under Rayleigh fading and shadowing," *Wireless Netw.*, vol. 22, no. 4, pp. 1285–1298, 2016.
- [15] H. Peng, D. Li, K. Abboud, H. Zhou, H. Zhao, W. Zhuang, and X. Shen, "Performance analysis of IEEE 802.11p DCF for multiplatforming communications with autonomous vehicles," *IEEE Trans. Veh. Technol.*, vol. 66, no. 3, pp. 2485–2498, Mar. 2017.
- [16] C. Han, M. Dianati, R. Tafazolli, R. Kernchen, and X. Shen, "Analytical study of the IEEE 802.11p MAC sublayer in vehicular networks," *IEEE Trans. Intell. Transp. Syst.*, vol. 13, no. 2, pp. 873–886, Jun. 2012.
- [17] K. Xu, D. Tipper, Y. Qian, and P. Krishnamurthy, "Time-dependent performance analysis of IEEE 802.11p vehicular networks," *IEEE Trans. Veh. Technol.*, vol. 65, no. 7, pp. 5637–5651, Jul. 2016.
- [18] J. Zheng and Q. Wu, "Performance modeling and analysis of the IEEE 802.11p EDCA mechanism for VANET," *IEEE Trans. Veh. Technol.*, vol. 65, no. 4, pp. 2673–2687, Apr. 2016.
- [19] Y. Hu, H. Li, Z. Chang, and Z. Han, "End-to-end backlog and delay bound analysis for multi-hop vehicular ad hoc networks," *IEEE Trans. Wireless Commun.*, vol. 16, no. 10, pp. 6808–6821, Oct. 2017.
- [20] M. Noor-A-Rahim, G. G. M. N. Ali, H. Nguyen, and Y. L. Guan, "Performance analysis of IEEE 802.11p safety message broadcast with and without relaying at road intersection," *IEEE Access*, vol. 6, pp. 23786–23799, 2018.
- [21] *IEEE Standard for Information Technology–Telecommunications and Information Exchange Between Systems Local and Metropolitan Area Networks–Specific Requirements Part 11: Wireless LAN Medium Access Control (MAC) and Physical Layer (PHY) Specifications*, IEEE Standard 802.11-2012, Mar. 2012, pp. 1–51.
- [22] M. I. Hassan, H. L. Vu, and T. Sakurai, "Performance analysis of the IEEE 802.11 MAC protocol for DSRC safety applications," *IEEE Trans. Veh. Technol.*, vol. 60, no. 8, pp. 3882–3896, Oct. 2011.
- [23] F. Bai and B. Krishnamachari, "Spatio-temporal variations of vehicle traffic in VANETs: Facts and implications," in *Proc. ACM Int. Workshop Veh. Internet Work.*, 2009, pp. 43–52.
- [24] X. M. Ma, X. Y. Yin, G. Butron, C. Penney, and K. S. Trivedi, "Packet delivery ratio in k-dimensional broadcast ad hoc networks," *IEEE Commun. Lett.*, vol. 17, no. 12, pp. 2252–2255, Dec. 2013.
- [25] F. Liu, J. Lin, Z. Tao, T. Korakis, E. Erkip, and S. Panwar, "The hidden cost of hidden terminals," in *Proc. IEEE ICC*, May 2010, pp. 1–6.
- [26] X. Ma, X. Chen, and H. H. Refai, "On the broadcast packet reception rates in one-dimensional MANETs," in *Proc. IEEE GLOBECOM*, Nov./Dec. 2008, pp. 1–5.
- [27] W. Zhang, "Analysis of packet forwarding in VANETs using probabilistic channel model," in *Proc. 69th IEEE Veh. Technol. Conf.*, Apr. 2009, pp. 1–5.
- [28] X. Ma and X. Chen, "Delay and broadcast reception rates of highway safety applications in vehicular ad hoc networks," in *Proc. Mobile Netw. Veh. Environ.*, May 2007, pp. 85–90.
- [29] L. Cheng, B. E. Henty, D. D. Stancil, F. Bai, and P. Mudalige, "Mobile vehicle-to-vehicle narrow-band channel measurement and characterization of the 5.9 GHz dedicated short range communication (DSRC) frequency band," *IEEE J. Sel. Areas Commun.*, vol. 25, no. 8, pp. 1501–1516, Oct. 2007.
- [30] Y. Yao, X. Chen, L. Rao, X. Liu, and X. Zhou, "LORA: Loss differentiation rate adaptation scheme for vehicle-to-vehicle safety communications," *IEEE Trans. Veh. Technol.*, vol. 66, no. 3, pp. 2499–2512, Mar. 2017.
- [31] Y. Yao, L. Rao, and X. Liu, "Performance and reliability analysis of IEEE 802.11p safety communication in a highway environment," *IEEE Trans. Veh. Technol.*, vol. 62, no. 9, pp. 4198–4212, Nov. 2013.
- [32] Y. Yao, L. Rao, X. Liu, and X. Zhou, "Delay analysis and study of IEEE 802.11p based DSRC safety communication in a highway environment," in *Proc. IEEE INFOCOM*, Apr. 2013, pp. 1591–1599.
- [33] F. J. Massey, Jr., "The Kolmogorov-Smirnov test for goodness of fit," *J. Amer. Statist. Assoc.*, vol. 46, no. 253, pp. 68–78, 1951.
- [34] L. H. Miller, "Table of percentage points of Kolmogorov statistics," *J. Amer. Stat. Assoc.*, vol. 51, no. 273, pp. 111–121, 1956.

[35] K. A. Hafeez, L. Zhao, B. Ma, and J. W. Mark, "Performance analysis and enhancement of the DSRC for VANET's safety applications," *IEEE Trans. Veh. Technol.*, vol. 62, no. 7, pp. 3069–3083, Sep. 2013.

[36] T. Sakurai and H. L. Vu, "MAC access delay of IEEE 802.11 DCF," *IEEE Trans. Wireless Commun.*, vol. 6, no. 5, pp. 1702–1710, May 2007.



**YUAN YAO** (M'15) received the B.S., M.S., and Ph.D. degrees in computer science from Northwestern Polytechnical University, Xi'an, China, in 2007, 2009, and 2015, respectively. Prior to joining the faculty at NPU, he was a Postdoctoral Researcher with the Department of Computing at Polytechnic University, Hong Kong. He is currently an Associate Professor with the School of Computer Science, Northwestern Polytechnical University. His research interests are in the area

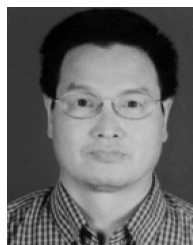
of real-time and embedded systems, cross-layer design in vehicular ad hoc networks, and safety in vehicular networks.



**YUJIAO HU** received the B.E. degree in computer science and technology from Northwestern Polytechnical University, Xi'an, China, in 2016, where she is currently pursuing the Ph.D. degree with the School of Computer Science and Engineering. Her current research interests include multiagent planning, coordination, and distributed control of complex systems, with application in unmanned aerial systems and cyber-physical environment.



**GANG YANG** received the B.E. degree from the School of Automation, Second Artillery Engineering College of PLA, Xi'an, China, in 1998, and the M.S. and Ph.D. degrees in computer science from Northwestern Polytechnical University, Xian, in 2002 and 2006, respectively, where he is currently a Professor with the School of Computer Science. His research interests include distributed computing systems, intelligent swarm systems, and cyber-physical systems.



**XINGSHE ZHOU** (M'04) received the B.S. and M.S. degrees in computer science from Northwestern Polytechnical University, Xi'an, China, where he is currently a Professor with the School of Computer Science. He is currently the Director of the Shaanxi Key Laboratory of Embedded System Technology, Xi'an. His research interests include embedded computing and pervasive computing.

...